

Hyperon Single-Particle Potentials Calculated from SU_6 Quark-Model Baryon-Baryon Interactions

M. Kohno, Y. Fujiwara*, T. Fujita*, C. Nakamoto** Y. Suzuki***

Physics Division, Kyushu Dental College, Kitakyushu 803-8580, Japan

**Department of Physics, Kyoto University, Japan*

***Suzuka National College of Technology, Suzuka 510-0294, Japan*

****Department of Physics, Niigata University, Niigata 950-2181, Japan*

Abstract

Using the SU_6 quark-model baryon-baryon interaction recently developed by the Kyoto-Niigata group, we calculate NN , ΛN and ΣN G -matrices in ordinary nuclear matter. This is the first attempt to discuss the Λ and Σ single-particle potentials in nuclear medium, based on the realistic quark-model potential. The Λ potential has the depth of more than 40 MeV, which is more attractive than the value expected from the experimental data of Λ -hypernuclei. The Σ potential turns out to be repulsive, the origin of which is traced back to the strong Pauli repulsion in the $\Sigma N(I = 3/2) \ ^3S_1$ state.

Key words: YN interaction, SU_6 quark model, G -matrix, hyperon single-particle potential

PACS: 13.75.Cs,12.39.Jh,13.75.Ev,24.85.+p

1 Introduction

The SU_6 quark-model provides a unified framework to describe baryon-baryon interactions including hyperons [1,2]. Recently the Kyoto-Niigata group has developed a modern quark-model baryon-baryon interaction [3–9], which reproduces essential features of the nucleon-nucleon (NN) and hyperon-nucleon (YN) scattering data below 300 MeV. In this model, the quark-quark interaction is assumed to consist of a phenomenological quark-confining potential, the Fermi-Breit interaction coming from the one-gluon exchange mechanism and effective meson-exchange potentials of scalar and pseudo-scalar meson nonets directly coupled to quarks. The interaction between the baryons is then derived

in a framework of $(3q)$ - $(3q)$ resonating-group method (RGM). The essential difference between the traditional meson-exchange potentials and the present quark model lies in a description of the short-range part of the interaction. In the traditional approach the baryon is treated as structureless and the short-range repulsion is introduced more or less phenomenologically with the aid of a hard-core, ω -meson exchange, or more recently pomeron-exchange between baryons. On the other hand, the compositeness of the baryon is explicitly considered in the quark Hamiltonian, and the origin of the short-range repulsion is the quark-exchange kernel of the color-magnetic term contained in the Fermi-Breit interaction, as well as the strong effect of the Pauli principle acting in some specific channels. Since the whole interaction acting between the baryons is determined by a strong cancellation between this repulsion at the short-range and the intermediate-range attraction, it is natural to expect that these two models predict quite different results for some observables whose experimental data are still not yet available. In fact, we have shown in the previous papers [7–9] that, in some YN observables and also in certain partial waves, the quark-model potential gives predictions different from that of the one-boson exchange model such as the Nijmegen model [10–13] and the Jülich model [14,15]. Since available experimental data are still scarce in the strangeness sector, it is useful to elucidate further the characteristics of the quark-model potential and to pursue its implications to hypernuclear physics.

Although the Λ single-particle (s.p.) potential in nuclei has been established experimentally [16], the Σ potential is basically unknown and even the sign of the Σ potential has been controversial [17]. Since there are no conclusive experimental data of the Σ hypernuclear states, a theoretical estimation of the Σ potential is made by extending known or unknown coupling constants to the Σ sector. The Nijmegen model D and soft-core potentials suggest an attractive Σ s.p. potential [18–20], while the Nijmegen model F indicates a repulsive one [19]. In a relativistic mean-field description [21], the results depend on the ratios of the coupling constants $\alpha_i \equiv (g_{i\Sigma^0}/g_{iN})$ ($i = \sigma, \omega, \rho$) which is not known a priori. Earlier studies [22], assuming a universal coupling, led to a Σ potential which is basically equal to the Λ one. A different choice of the ratios was found later [23] to be able to give a repulsive Σ potential. In view of the fact that various models give different predictions, it is interesting to discuss theoretical predictions of the Σ potential obtained from a quark model which unifies a description of NN and YN interactions.

In this paper we present G -matrix calculations, in the lowest order Brueckner theory [24,25], for the NN , ΛN and ΣN interactions in ordinary nuclear matter, by using the quark-model interaction developed by the Kyoto-Niigata group. There are several versions of the quark model; RGM-F [3,4], FSS [5–9] and RGM-H [6–9]. We report mainly the results with the FSS, since it incorporates the effective meson-exchange potentials in the complete microscopic way. Although Λp total cross section in the cusp region is somewhat overesti-

mated due to the strong antisymmetric LS force ($LS^{(-)}$ force), the threshold energy of the ΣN channel is correctly reproduced. We discuss nuclear-matter saturation properties and s.p. potentials of the N , Λ and Σ obtained from the G -matrices. These properties predicted by the other versions of our quark model, RGM-F and RGM-H, are essentially the same. Further analysis of partial-wave contributions enables us to clarify general characteristics of our quark model.

The problem of the strength of the hyperon s.p. spin-orbit potential is another interesting and important issue. The analysis on this subject based on the quark-model G -matrices is treated in a separate paper [26].

We outline in Section 2 a calculation of G -matrices from the quark-model baryon-baryon interactions. The saturation property of nuclear matter, predicted by the model FSS, is discussed in Section 3. Hyperon s.p. potentials in nuclear matter are discussed in Section 4. Summary is drawn in Section 5.

2 G -matrices of the quark-model potential

The quark-model interaction is defined through the RGM equation for the parity-projected relative wave function $\chi_\alpha(\mathbf{R})$ of the $(3q)$ - $(3q)$ clusters:

$$\left[\varepsilon_\alpha + \frac{\hbar^2}{2\mu_\alpha} \left(\frac{\partial}{\partial \mathbf{R}} \right)^2 \right] \chi_\alpha(\mathbf{R}) = \sum_{\alpha'} \int d\mathbf{R}' G_{\alpha,\alpha'}(\mathbf{R}, \mathbf{R}'; E) \chi_\alpha(\mathbf{R}') . \quad (1)$$

The subscript α specifies a set of quantum numbers of the channel wave function, $\alpha = [1/2(11)a_1, 1/2(11)a_2] \text{ } SS_z YII_z; \mathcal{P}$, where \mathcal{P} is the flavor-exchange phase and $1/2(11)a$ denotes the spin, the SU_3 quantum number in the Elliott notation ($\lambda\mu$), and the flavor label $a = YI$ of the octet baryons, respectively. For example, $YI = 1(1/2)$ for N , 00 for Λ , and 01 for Σ . The relative energy ε_α of the channel α is related to the total energy E of the system through $\varepsilon_\alpha = E - E_{a_1}^{int} - E_{a_2}^{int}$ with $E_{a_i}^{int}$ being the intrinsic energy of the baryon. The exchange kernel $G_{\alpha\alpha'}(\mathbf{R}, \mathbf{R}'; E)$ is given by

$$G_{\alpha\alpha'}(\mathbf{R}, \mathbf{R}'; E) = \delta(\mathbf{R} - \mathbf{R}') \left[\sum_{\beta} V_{\alpha\alpha'D}^{(CN)\beta}(\mathbf{R}) + \sum_{\beta} V_{\alpha\alpha'D}^{(SN)\beta}(\mathbf{R}) \right. \\ \left. + \sum_{\beta} V_{\alpha\alpha'D}^{(TN)\beta}(\mathbf{R}) (S_{12})_{\alpha\alpha'} \right] + \sum_{\Omega} \mathcal{M}_{\alpha\alpha'}^{(\Omega)}(\mathbf{R}, \mathbf{R}') - \varepsilon_\alpha \mathcal{M}_{\alpha\alpha'}^N(\mathbf{R}, \mathbf{R}') . \quad (2)$$

The quark exchange kernel $\mathcal{M}_{\alpha\alpha'}^{(\Omega)}(\mathbf{R}, \mathbf{R}')$ on the right hand side of Eq.(2) includes a sum over $\Omega = K$ for the exchange kinetic-energy kernel, various pieces of the Fermi-Breit interaction, as well as CN for the central term of the scalar- (S-) meson exchange, SN for the spin-spin term of the pseudo-scalar- (PS-) meson exchange, and TN for the tensor term of the PS-meson exchange. For details, [3] and [6] should be referred to. According to [27], we introduce the basic Born kernel of Eq.(2) through

$$M_{\alpha\alpha'}(\mathbf{q}_f, \mathbf{q}_i; E) = \langle e^{i\mathbf{q}_f \cdot \mathbf{R}} | G_{\alpha\alpha'}(\mathbf{R}, \mathbf{R}'; E) | e^{i\mathbf{q}_i \cdot \mathbf{R}'} \rangle . \quad (3)$$

The full Born kernel of the quark-exchange kernel is given by

$$V_{\gamma\alpha}(\mathbf{p}, \mathbf{q}; E) = \frac{1}{2} \left[M_{\gamma\alpha}(\mathbf{p}, \mathbf{q}; E) + (-1)^{S_\alpha} \mathcal{P}_\alpha M_{\gamma\alpha}(\mathbf{p}, -\mathbf{q}; E) \right] . \quad (4)$$

It is now straightforward to convert the RGM equation Eq.(1) to the Lippmann-Schwinger-type equation [28], which takes the form

$$\begin{aligned} T_{\gamma\alpha}(\mathbf{p}, \mathbf{q}; E) &= V_{\gamma\alpha}(\mathbf{p}, \mathbf{q}; E) + \sum_{\beta} \frac{1}{(2\pi)^3} \int d\mathbf{k} V_{\gamma\beta}(\mathbf{p}, \mathbf{k}; E) \\ &\times \frac{2\mu_{\beta}}{\hbar^2} \frac{1}{k_{\beta}^2 - k^2 + i\varepsilon} T_{\beta\alpha}(\mathbf{k}, \mathbf{q}; E) . \end{aligned} \quad (5)$$

Here the total energy E is related to k_{β}^2 through $E = \varepsilon_{\beta} + E_{b_1}^{int} + E_{b_2}^{int}$ with $\varepsilon_{\beta} = (\hbar^2 k_{\beta}^2 / 2\mu_{\beta})$.

The Bethe-Goldstone (BG) equation for the G -matrix solution is obtained by replacing the propagator in Eq.(5) as

$$\frac{2\mu_{\beta}}{\hbar^2} \frac{1}{k_{\beta}^2 - k^2 + i\varepsilon} \rightarrow \frac{Q_{\beta}(k, K)}{e_{\beta}(k, K; \omega)} , \quad (6)$$

where $Q_{\beta}(k, K)$ stands for the angle-averaged Pauli operator and $e_{\beta}(k, K; \omega)$ is the energy denominator given by¹

$$e_{\beta}(k, K; \omega) = \omega - E_b(k_1) - E_N(k_2) . \quad (7)$$

Explicit expressions for Q_{β} and k_i are discussed below. First $E_b(k)$ is the s.p. energy defined through

$$E_b(k) = M_b + \frac{\hbar^2}{2M_b} k^2 + U_b(k) , \quad (8)$$

¹ For s.p. potentials, we use the notation $b_1 = b$ and $a_1 = a$ to specify baryons.

with $U_b(k)$ and M_b being the s.p. potential and the mass for the baryon b , respectively.² The starting energy ω is a sum of the s.p. energies of two interacting baryons:

$$\begin{aligned}\omega &= E_a(k_1) + E_N(k_2) \\ &= M_a + M_N + \frac{\hbar^2}{2(M_a + M_N)} K^2 + \frac{\hbar^2}{2\mu_\alpha} q^2 + U_a(k_1) + U_N(k_2) \quad ,\end{aligned}\quad (9)$$

where \mathbf{K} and \mathbf{q} are the total and relative momenta corresponding to the initial s.p. momenta \mathbf{k}_1 and \mathbf{k}_2 . The BG equation is, therefore, expressed as

$$\begin{aligned}G_{\gamma\alpha}(\mathbf{p}, \mathbf{q}; \omega) &= V_{\gamma\alpha}(\mathbf{p}, \mathbf{q}; E) + \sum_\beta \frac{1}{(2\pi)^3} \int d \mathbf{k} V_{\gamma\beta}(\mathbf{p}, \mathbf{k}; E) \\ &\quad \times \frac{Q_\beta(k, K)}{e_\beta(k, K; \omega)} G_{\beta\alpha}(\mathbf{k}, \mathbf{q}; \omega) \quad ,\end{aligned}\quad (10)$$

and the s.p. potential is calculated from

$$\begin{aligned}U_a(k_1) &= \sum_{\sigma_2, \tau_2} \int_{|\mathbf{k}_2| < k_F} d \mathbf{k}_2 \langle a \mathbf{k}_1 N \mathbf{k}_2 | \\ &\quad \times G(\omega = E_a(k_1) + E_N(k_2)) | a \mathbf{k}_1 N \mathbf{k}_2 - N \mathbf{k}_2 a \mathbf{k}_1 \rangle \quad ,\end{aligned}\quad (11)$$

with k_F being the Fermi-momentum of symmetric nuclear matter. In Eq. (11) the sum over σ_2, τ_2 implies the spin-isospin sum with respect to the nucleons in nuclear matter.

There exists an inherent ambiguity of how to deal with the energy dependence of the Born kernel $V_{\gamma\alpha}(\mathbf{p}, \mathbf{q}; E)$ in the BG equation Eq. (10). The total energy of the two interacting particles in the nuclear medium is not conserved. Since we only need the diagonal G -matrices for calculating s.p. potentials, we here simply use

$$\varepsilon_\gamma = E_a^{int} - E_c^{int} + \frac{\hbar^2}{2\mu_\alpha} q^2 \quad ,\quad (12)$$

both in $V_{\gamma\alpha}(\mathbf{p}, \mathbf{q}; E)$ and $V_{\gamma\beta}(\mathbf{p}, \mathbf{k}; E)$ in Eq. (10).

We use two different assumptions for the s.p. potentials involved in $E_b(k_1) + E_N(k_2)$ term of Eq. (7). The first one is the so-called QTQ prescription defined by taking only the rest mass and kinetic-energy term in Eqs. (7) and (8).

² It should be noted that $M_b = E_b^{int}$ since the threshold energy is usually fitted to the experimental value in our model.

The other case, the continuous choice, is given by the s.p. potential calculated self-consistently. If the energy denominator $e_\beta(k, K; \omega)$ involves a pole, the solution of the BG equation becomes complex, so does the s.p. potential $U_a(q_1)$ in Eq. (11). In this case, only the real part $\text{Re } U_b(k)$ is retained in $e_\beta(k, K; \omega)$. As for the Pauli operator $Q_\beta(k, K)$, we adopt the standard angle-average approximation. Denoting the mass, the momentum and the Fermi momentum of the one particle by M_1 , \mathbf{k}_1 and $k_F^{(1)}$ and those of the other by M_2 , \mathbf{k}_2 and $k_F^{(2)}$, the angle-averaged Pauli operator for the total and relative momenta of $\mathbf{K} = \mathbf{k}_1 + \mathbf{k}_2$ and $\mathbf{k} = (\xi \mathbf{k}_1 - \mathbf{k}_2)/(1 + \xi)$ with $\xi = (M_2/M_1)$ is given by

$$Q_\beta(k, K) = \frac{1}{2} \int_{-1}^1 d \cos \theta \times \Theta \left(\left| \frac{1}{1 + \xi} \mathbf{K} + \mathbf{k} \right| - k_F^{(1)} \right) \Theta \left(\left| \frac{\xi}{1 + \xi} \mathbf{K} - \mathbf{k} \right| - k_F^{(2)} \right), \quad (13)$$

where Θ is the Heaviside's step function and θ denotes the angle between \mathbf{K} and \mathbf{k} . This becomes

$$\begin{aligned} Q_\beta(k, K) &= [0] \left([-1|z_1|1] + [-1|z_2|1] \right) / 2|1] , \\ z_1 &= \frac{1}{2} (1 + \xi) \frac{1}{kK} \left\{ \left(\frac{1}{1 + \xi} K \right)^2 + k^2 - (k_F^{(1)})^2 \right\} , \\ z_2 &= \frac{1}{2} \left(1 + \frac{1}{\xi} \right) \frac{1}{kK} \left\{ \left(\frac{\xi}{1 + \xi} K \right)^2 + k^2 - (k_F^{(2)})^2 \right\} , \end{aligned} \quad (14)$$

where we have introduced the notation $[a|b|c] \equiv \max(a, \min(b, c))$ as is used in [20]. For the YN system, we set $k_F^{(1)} = 0$ and $k_F^{(2)} = k_F$, which results in $Q_\beta(k, K) = (1 + [-1|z_0|1])/2$ with

$$z_0 = \frac{1}{2} \left(1 + \frac{1}{\xi} \right) \frac{1}{kK} \left[\left(\frac{\xi}{1 + \xi} K \right)^2 + k^2 - k_F^2 \right] . \quad (15)$$

For the NN system, $k_F^{(1)} = k_F^{(2)} = k_F$ yields $Q_\beta(k, K) = [0|z_0|1]$ with $\xi = 1$.

It is convenient to deal with partial-wave components of the Born kernel, by carrying out angular integration numerically. We define $V_{\gamma S' \ell', \alpha S \ell}^J(p, q; E)$ through

$$V_{\gamma \alpha}(\mathbf{p}, \mathbf{q}; E) = \sum'_{JM \ell \ell'} 4\pi V_{\gamma S' \ell', \alpha S \ell}^J(p, q; E)$$

$$\times \sum_{m'} \langle \ell' m' S' S'_z | JM \rangle \, Y_{\ell' m'}(\hat{\mathbf{p}}) \, \sum_m \langle \ell m S S_z | JM \rangle \, Y_{\ell m}^*(\hat{\mathbf{q}}) \quad , \quad (16)$$

where $\gamma = [1/2(11)c_1, 1/2(11)c_2] \, S' S'_z YII_z; \mathcal{P}'$, and the prime in \sum' indicates that the sum over ℓ and ℓ' is only for $(-1)^{S'} \mathcal{P}' = (-1)^{\ell'} = (-1)^S \mathcal{P} = (-1)^{\ell} =$ parity. Then it is straightforward to apply Eq. (16) to the partial-wave decomposition [29] of the BG equation in nuclear matter:

$$\begin{aligned} G_{\gamma S' \ell', \alpha S \ell}^J(p, q; K, \omega) &= V_{\gamma S' \ell', \alpha S \ell}^J(p, q; E) + \frac{4\pi}{(2\pi)^3} \sum'_{\beta S'' \ell''} \int_0^\infty k^2 dk \, k \\ &\times V_{\gamma S' \ell', \beta S'' \ell''}^J(p, k; E) \frac{Q_\beta(k, K)}{e_\beta(k, K; \omega)} \, G_{\beta S'' \ell'', \alpha S \ell}^J(k, q; K, \omega) \quad . \end{aligned} \quad (17)$$

The s.p. potential is calculated from

$$\begin{aligned} U_a(k_1) &= (1 + \delta_{a,N}) \sum_I \frac{2I + 1}{2(2I_a + 1)} \\ &\times \sum_{J \ell S} (2J + 1) \frac{1}{(2\pi)^2} \int_{-1}^1 d \cos \theta_2 \int_0^{k_F} k_2^2 dk_2 \, G_{a S \ell, a S \ell}^J(q, q; K, \omega) \quad , \end{aligned} \quad (18)$$

where q , K and ω are given by

$$\begin{aligned} q &= \frac{1}{1 + \xi} \left[\xi^2 k_1^2 + k_2^2 - 2\xi k_1 k_2 \cos \theta_2 \right]^{\frac{1}{2}} \quad , \quad \xi = \frac{M_N}{M_a} \quad , \\ K &= \left[k_1^2 + k_2^2 + 2k_1 k_2 \cos \theta_2 \right]^{\frac{1}{2}} \quad , \\ \omega &= E_a(k_1) + E_N(k_2) \quad . \end{aligned} \quad (19)$$

If we average the K -dependence of the G -matrix, the calculation can be further simplified. Changing the integral variable to the relative momentum \mathbf{q} , the expression for the $U_a(k_1)$ becomes

$$\begin{aligned} U_a(k_1) &= (1 + \delta_{a,N})(1 + \xi)^3 \sum_I \frac{2I + 1}{2(2I_a + 1)} \\ &\times \sum_{J \ell S} (2J + 1) \frac{1}{2\pi^2} \int_0^{q_{max}} q^2 dq \, W(k_1, q) \, G_{a S \ell, a S \ell}^J(q, q; K, \omega) \quad , \end{aligned} \quad (20)$$

where $q_{max} = (k_F + \xi k_1)/(1 + \xi)$, and $W(k_1, q)$ is the phase space factor given by

$$W(k_1, q) = \frac{1}{2} (1 - [-1|x_0|1]) \quad \text{with} \quad x_0 = \frac{\xi^2 k_1^2 + (1 + \xi)^2 q^2 - k_F^2}{2\xi(1 + \xi)k_1 q} . \quad (21)$$

Once k_1 and q are given, the values of K , k_2 and ω are calculated through

$$\begin{aligned} K &= (1 + \xi) \left[k_1^2 + q^2 - k_1 q (1 + [-1|x_0|1]) \right]^{\frac{1}{2}} , \\ k_2 &= \left[\frac{\xi}{1 + \xi} K^2 + (1 + \xi) q^2 - \xi k_1^2 \right]^{\frac{1}{2}} , \\ \omega &= E_a(k_1) + E_N(k_2) . \end{aligned} \quad (22)$$

In Eqs. (21) and (22), we should assume $x_0 = -1$ when $k_1 = 0$.

In the continuous prescription, we need to determine the s.p. momenta k_1 and k_2 in Eq. (7) for the intermediate energy spectra. These are given through

$$\begin{aligned} k_1^2 &= \left(\frac{1}{1 + \xi} K \right)^2 + k^2 + \frac{1}{1 + \xi} k K ([-1|z_2|1] - [-1|z_1|1]) , \\ k_2^2 &= \left(\frac{\xi}{1 + \xi} K \right)^2 + k^2 - \frac{\xi}{1 + \xi} k K ([-1|z_2|1] - [-1|z_1|1]) , \end{aligned} \quad (23)$$

in the two Fermi-sphere case. For the NN system, there is a special situation that the linear term of z vanishes in the process of angular averaging. In this case, we use the angle-average over z^2 , as is discussed in [20], and use

$$\begin{aligned} k_1^2 &= \frac{1}{4} K^2 + k^2 + k K \frac{1}{\sqrt{3}} [0|z_0|1] , \\ k_2^2 &= \frac{1}{4} K^2 + k^2 - k K \frac{1}{\sqrt{3}} [0|z_0|1] , \end{aligned} \quad (24)$$

where z_0 is given by Eq. (15) with $\xi = 1$.

Finally, the ground-state energy per nucleon of symmetric nuclear matter is given by

$$\frac{E}{A} = \frac{3}{5} \left(\frac{\hbar^2}{2M_N} k_F^2 \right) + \frac{3}{2k_F^3} \int_0^{k_F} k^2 d k U_N(k) . \quad (25)$$

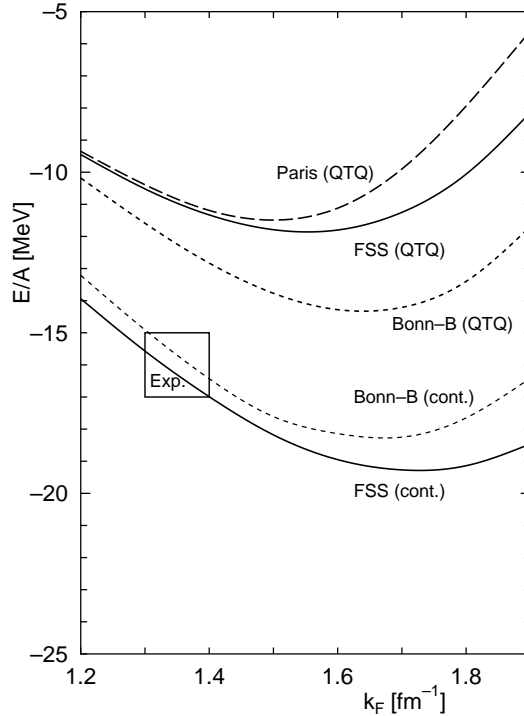


Fig. 1. Nuclear matter saturation curves obtained for the quark-model potential FSS, together with the results with the Paris potential [30] and the Bonn potential [31]. The choice of the intermediate spectra is specified by "QTQ" and "cont.", respectively. The result for the Bonn-B potential with the continuous choice is taken from the nonrelativistic calculation in [32].

3 Saturation properties of nuclear matter

Figure 1 shows saturation curves calculated for ordinary nuclear matter with the QTQ prescription as well as the continuous choice for intermediate spectra, together with the results of the Paris potential [30] and the Bonn B potential [31]. The k -dependence of the nucleon s.p. potential $U_N(k)$ obtained with the continuous choice is shown in Fig. 2 at three densities $\rho = 0.5\rho_0$, $0.7\rho_0$ and ρ_0 with the normal density $\rho_0 = 0.17 \text{ fm}^{-3}$, which correspond to $k_F = 1.07$, 1.2 , 1.35 fm^{-1} . For comparison, the result with the Nijmegen soft-core (NSC) potential NSC89 [12] calculated by Schulze *et al.* [20] is also shown. At lower momentum, $k < 2k_F$, our result is close to the potential obtained with the NSC NN potential.

In the calculation with the continuous prescription, it turns out that the nucleon s.p. potential starts to decrease at $k \sim 4 \text{ fm}^{-1}$, the tendency of which is seen in Fig. 2. This behavior of the s.p. potential suggests that the short-range repulsion of the NN interaction in the FSS may not be strong enough at higher energies, namely beyond the region where the parameters are fixed to reproduce the scattering data. Actually, this is not the case since the NN differential

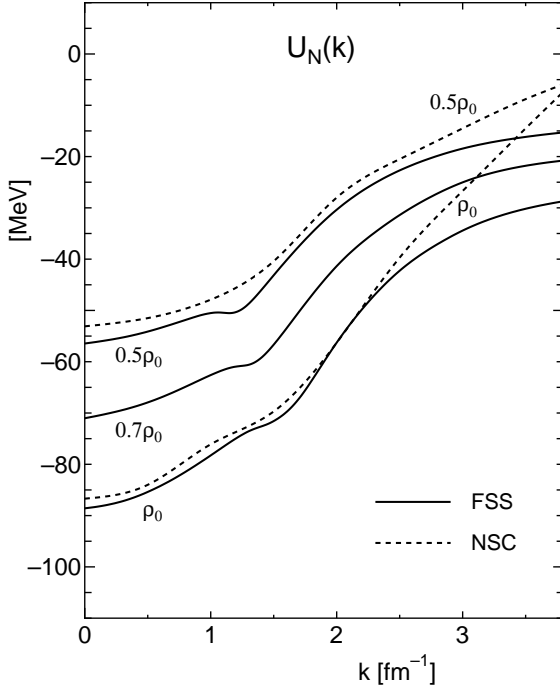


Fig. 2. The nucleon s.p. potential $U_N(k)$ in nuclear matter with the continuous choice for intermediate spectra. The quark model is FSS. Potentials for three densities of $\rho = 0.5\rho_0, 0.7\rho_0, \rho_0$ are shown, where the normal density ρ_0 corresponds to $k_F = 1.35 \text{ fm}^{-1}$. The dashed curve is the result by Schulze *et al.* [20] with the Nijmegen soft-core NN potential NSC89 [12].

cross sections are not largely overestimated at higher energy region even up to 800 MeV [33]. Detailed analysis [28] implies that this particular feature of FSS is caused by the ill-behavior of the spin-independent central invariant amplitude at the forward angles, which is intimately related to the asymptotic behavior of s.p. potentials in the high-momentum region. This flaw of the model FSS may be removed by introducing the momentum-dependent higher-order term involved in the S-meson exchange central force. In the present application, we introduced an ad hoc prescription to set $U_N(k) = U_N(k = 3.8 \text{ fm}^{-1})$ for $k \geq 3.8 \text{ fm}^{-1}$ in case of the continuous choice for the intermediate spectra.³ Since the kinetic energy term dominates at higher energies, the result does not depend much on this particular prescription.

The short-range part of the FSS is mainly described by the quark-exchange mechanism. The non-local character of this part is different from the usual vector meson exchange picture in the one-boson exchange model. In spite of the difference the saturation point of the quark-model FSS is seen not to deviate from the Coester band, which indicates that the FSS has similar saturation properties with other realistic meson-exchange potentials.

³ The value of $k = 3.8 \text{ fm}^{-1}$ corresponds to the incident energy $T_{lab} = 300 \text{ MeV}$ in the two-nucleon scattering.

4 Hyperon potentials in nuclear matter

For hyperon s.p. potentials in nuclear matter, we show the results with the continuous prescription for intermediate spectra. Since the Λ and Σ are coupled in the isospin $I = 1/2$ channel, these potentials are calculated self-consistently. Since the asymptotic behavior in the high-momentum region seems to be unsatisfactorily described as in the case of the NN channel, the same prescription in the energy denominator as for the nucleon is introduced; namely, $U_\Lambda(k) = U_\Lambda(k = 3.8 \text{ fm}^{-1})$ and $U_\Sigma(k) = U_\Sigma(k = 3.8 \text{ fm}^{-1})$ for $k \geq 3.8 \text{ fm}^{-1}$.

4.1 Λ s.p. potential

Figs. 3 shows the momentum dependence of the Λ s.p. potential in nuclear matter obtained from quark-model G -matrices. For comparison, the result by Schulze *et al.* [20] with the NSC YN potential NSC89 [12] is also shown. Partial wave contributions of the s.p. potential $U_\Lambda(k = 0)$ in nuclear matter at $k_F = 1.35 \text{ fm}^{-1}$ are tabulated in Table 1.

The FSS is seen to produce a larger potential depth $U_\Lambda(0)$ than the NSC. Actually the depth of 46 MeV in the case of $k_F = 1.35 \text{ fm}^{-1}$ is larger than that of the standard phenomenological potential depth of about 30 MeV [16]. It is, however, necessary to consider the density dependence of the potential in

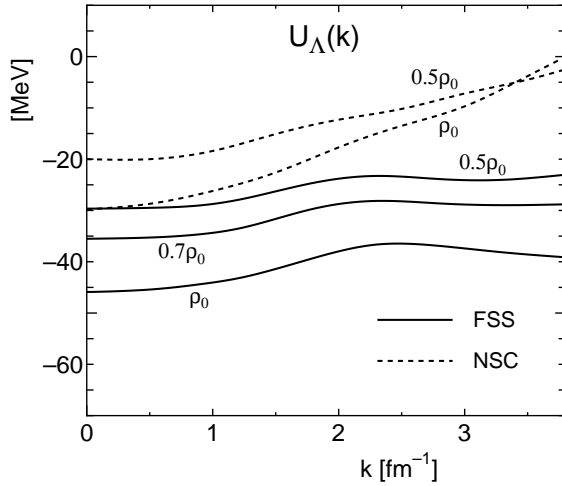


Fig. 3. The Λ s.p. potential $U_\Lambda(k)$ in symmetric nuclear matter with the continuous choice for intermediate spectra. The quark model is FSS. Potentials for three densities of $\rho = 0.5\rho_0, 0.7\rho_0, \rho_0$ are shown, where the normal density ρ_0 corresponds to $k_F = 1.35 \text{ fm}^{-1}$. The dashed curve is the result by Schulze *et al.* [20] with the Nijmegen soft-core YN potential NSC89 [12].

Table 1

Λ and Σ s.p. potentials in nuclear matter with $k_F = 1.35$ fm $^{-1}$, calculated from our quark-model (FSS) G -matrices with the continuous prescription for intermediate spectra. Predictions by Nijmegen soft-core potential (NSC) [12] is also shown for comparison [20].

	$U_\Lambda(0)$ [MeV]		$U_\Sigma(0)$ [MeV]			
	FSS	NSC	FSS	NSC		
I	1/2	1/2	1/2	3/2	1/2	3/2
1S_0	-19.9	-15.3	6.1	-8.8	6.7	-12.0
$^3S_1 + ^3D_1$	-21.2	-13.0	-19.7	48.3	-14.9	6.7
$^1P_1 + ^3P_1$	0.2	3.6	-6.7	4.0	-3.5	3.9
3P_0	0.6	0.2	3.0	-2.3	2.6	-2.0
$^3P_2 + ^3F_2$	-4.6	-4.0	-1.2	-1.2	-0.5	-1.9
subtotal			-21.0	41.4	-9.8	-5.5
total	-45.9	-29.8		+20.7		-15.3

order to relate $U_\Lambda(0)$ to the empirical potential in finite nuclei. The correction from the starting energy dependence also modifies the s.p. potential.

If we compare the FSS and NSC results in Table 1, we find that the additional attraction of our $U_\Lambda(0)$ to the NSC originates from three sources; 1) about 5 MeV excess for 1S_0 state, 2) about 8 MeV excess for $^3S_1 + ^3D_1$ state, and 3) about 3 MeV excess for $^1P_1 + ^3P_1$ state. The first one is apparently because our ΛN 1S_0 state is too attractive as is seen from the phase-shift behavior shown in Fig. 4 of [6]. The detailed analysis of the s -shell Λ -hypernuclei seems to imply that the relative strength of the attraction of the 1S_0 and 3S_1 states is most desirable to be such that the maximum peak of the 1S_0 phase shift is larger than that of 3S_1 by about 10° [34–36]. If we fit the available low-energy Λp total cross section data, this condition yields $\delta_{max}(^1S_0) \sim 34^\circ - 36^\circ$ and $\delta_{max}(^3S_1) \sim 26^\circ$ approximately. On the other hand, the FSS (and also RGM-H) prediction is $\delta_{max}(^1S_0) \sim 46^\circ$ and $\delta_{max}(^3S_1) \sim 17^\circ$, and our 1S_0 state is too attractive. For the contribution 2), it is a puzzle why these low values of the 3S_1 phase shift give such a large attractive contribution as -21.2 MeV. It can be checked by switching off the $\Lambda N - \Sigma N$ transition interaction that about a half of the attractive contribution comes through the $\Lambda N - \Sigma N$ coupling.

As to the contribution 3), we should note that P -state interaction of our quark model is weakly attractive in the low-energy region, because of a very strong effect of the antisymmetric LS force ($LS^{(-)}$ force) [9]. Among many versions of the Nijmegen models, only the model D gives attractive P -wave interaction. However, the mechanism of producing the attraction is entirely different between our model and the model D. In our case, a very strong $\Lambda N - \Sigma N$ ($I = 1/2$) coupling takes place around the ΣN threshold region in

the $^1P_1 + ^3P_1$ state, which is due to the $LS^{(-)}$ force originating from the Fermi-Breit spin-orbit interaction. A broad P -state resonance exists either in the $\Sigma N(I = 1/2)$ 3P_1 state or in the ΛN 1P_1 state, depending on the strengths of the coupling matrix elements and of the central attraction in the $\Sigma N(I = 1/2)$ channel. The 1P_1 and 3P_1 phase shifts become attractive even at $p_{lab} = 300$ MeV/c by the influence of this resonance. This attractive behavior of the Λp P -wave interaction can be examined experimentally by observing the forward-to-backward ratio of the Λp differential cross sections in the $p_{lab} \leq 300$ MeV/c region [9].

Figure 3 also indicates that the momentum dependence of the Λ s.p. potential is weak. If we define a global effective mass by

$$\frac{m^*(k)}{m} = \left[1 + \frac{2m}{\hbar^2 k^2} (U(k) - U(0)) \right]^{-1} \quad (26)$$

$m^*(k \sim 1 \text{ fm}^{-1})/m \sim 0.90, 0.94$ and 0.95 at $k_F = 1.35, 1.2$ and 1.07 fm^{-1} , respectively, which is larger than that of the nucleon of $0.66, 0.72$ and 0.79 at the corresponding k_F . The potential from the NSC is also seen to show a flat k -dependence similar to the FSS. Supposing that the interaction G in eq. (11) is a local two-body potential, the direct term does not give k -dependence and the exchange term, which is a strangeness exchange process, is the origin of the effective mass. Although the two-body correlation together with the Pauli operator Q in the BG equation brings about the momentum dependence even in the direct term, the chief source of the effective mass in the hyperon s.p. potential is considered to be the strangeness exchange process. The possible reason for the difference of the lambda and nucleon effective masses is the absence of the long-ranged one-pion exchange in the Λ case.

The imaginary part of the Λ s.p. potential is shown in Fig. 4. The imaginary part comes from creating a nucleon one-particle-one-hole state. Since only the nucleons near the Fermi surface participate for inelastic processes of the Λ 's having small k , the imaginary strength is small for these lambda states, which corresponds to the small spreading width of the Λ formation peaks observed in (K, π) and (π, K) reactions [37].

4.2 Σ s.p. potential

The momentum dependence of the Σ s.p. potential is shown in Fig. 5. The result by Schulze *et al.* [20] with the NSC YN potential NSC89 [12] is also shown. The $U_\Sigma(k = 0)$ turns out to be positive, which is a marked difference from the results of other YN potentials except for the Nijmegen model F. Table 1 presents each partial wave contribution to the $U_\Sigma(0)$, which shows the

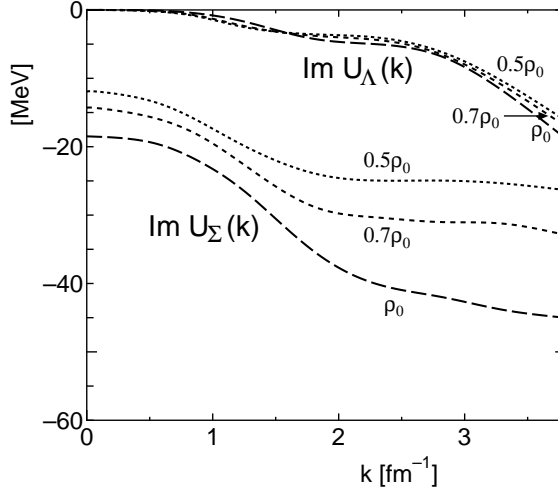


Fig. 4. The imaginary part of the Λ and Σ s.p. potentials $U_a(k)$ in symmetric nuclear matter with the continuous choice for intermediate spectra. The quark model is FSS. Potentials for three nuclear matter densities of $\rho = 0.5\rho_0, 0.7\rho_0, \rho_0$ are shown, where the normal density ρ_0 corresponds to $k_F = 1.35 \text{ fm}^{-1}$.

strong repulsive contribution in $I = 3/2 \ ^3S_1 + \ ^3D_1$ channel. This repulsion is a direct result of the strong quark-antisymmetrization effect in this particular channel [6].

Since the repulsive Σ s.p. potential is not common with many other realistic YN potentials, it would be useful to examine predictions by the other versions of our quark model, RGM-F and RGM-H. Because of a technical reason, it is not possible to obtain a reasonable s.p. potential for Λ in these models. The completely Pauli-forbidden $(11)_s$ component in the ΛN - ΣN ($I = 1/2$) coupled-channel system is not exactly eliminated in the present calculation. In the ΛN scattering, this causes an unrealistic ΛN - ΣN coupling in the 1S_0 state, which was remedied in the previous variational calculation by modifying

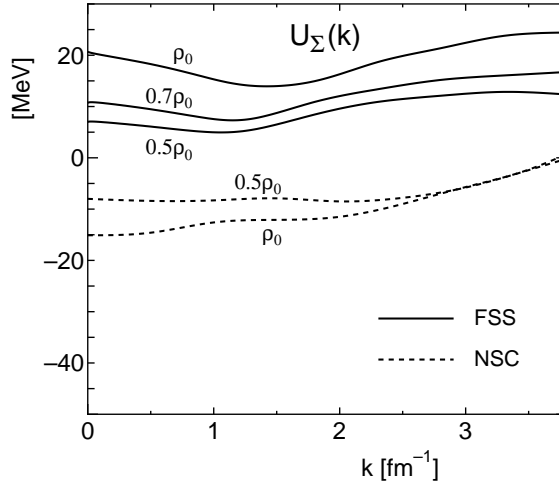


Fig. 5. The same as Fig. 3 but for the Σ s.p. potential $U_\Sigma(k)$.

the spin-flavor factors for this particular channel [4]. It is, however, not easy to incorporate this prescription in the Lippmann-Schwinger and G -matrix equations, since these equations are formulated in the momentum representation. Without this prescription, the inaccuracy of the ΛN 1S_0 phase shift sometimes reaches at more than 10 degrees. This is because the antisymmetrization of the effective-meson exchange potentials is not exactly treated in these models.⁴ In spite of these difficulties, we believe that the Σ s.p. potentials are rather correctly calculated, since the phase-shift behavior of the ΣN channel is fairly similar between the two cases with this prescription and without this prescription.

Table 2 shows partial-wave contributions of $U_\Sigma(0)$ in nuclear matter at $k_F = 1.35 \text{ fm}^{-1}$, predicted by our three versions RGM-F, FSS and RGM-H. Here we exceptionally used completely self-consistent s.p. potentials $U_B(k)$ ($B = N, \Lambda, \Sigma$), without introducing any cut-off at $k = 3.8 \text{ fm}^{-1}$, for the intermediate spectra in the continuous prescription. We also employed the approximate angular integration in Eq.(20). We find that the difference of the FSS prediction in Table 1 and Table 2 is very small. It is a common feature for the three versions that they give similarly strong repulsion in the $\Sigma N(I = 3/2)$ $^3S_1 + ^3D_1$ state. It may look strange that $\Sigma N(I = 1/2)$ 1S_0 state gives only weak repulsion in all these three versions, in spite of the fact that the phase-shift behavior of this channel is almost comparably repulsive to the $\Sigma N(I = 3/2)$ $^3S_1 + ^3D_1$ channel. On the other hand, the

⁴ The same problem exists even in the model FSS with respect to the exchange kinetic-energy kernel. However, the effect to the phase shift is very small and the phase-shift difference is less than 2 degrees.

Table 2

Σ s.p. potentials in nuclear matter at $k_F = 1.35 \text{ fm}^{-1}$, calculated from our three versions of the quark model; RGM-H [4], FSS [5,6], and RGM-H [6]. The completely self-consistent s.p. potentials are used with the continuous prescription for intermediate spectra, together with Eq.(20).

I	$U_\Sigma(0)$ [MeV]						
	RGM-F			FSS		RGM-H	
	1/2	3/2	1/2	3/2	1/2	3/2	
1S_0	5.4	-10.7	6.0	-8.8	9.3	-13.6	
$^3S_1 + ^3D_1$	-25.4	43.5	-20.7	47.5	-17.9	39.1	
$^1P_1 + ^3P_1$	-10.8	4.8	-7.7	3.9	-8.1	1.6	
3P_0	3.2	-3.3	2.9	-2.3	2.7	-2.4	
$^3P_2 + ^3F_2$	-2.1	-5.0	-1.3	-1.2	-1.7	-3.8	
subtotal	-31.8	30.0	-22.3	40.0	-17.5	21.0	
total		-1.9		+17.6		+3.5	

attractive behavior of the $\Sigma N(I = 3/2)$ 1S_0 and $\Sigma N(I = 1/2)$ $^3S_1 + ^3D_1$ channels reflects the characteristics of each version very well. Namely, the low-energy behavior of the $\Sigma N(I = 3/2)$ 1S_0 phase shift in RGM-H is too attractive, corresponding to the slight over-estimation of the $\Sigma^+ p$ total elastic cross sections at $p_{lab} \leq 300$ MeV/c (see Fig. 11(a) of [6]). In the $\Sigma N(I = 1/2)$ $^3S_1 + ^3D_1$ channel, it is discussed in [28] and [38] that the central attraction becomes weaker for RGM-F, FSS and RGM-H in this order. As a measure of this strength, we calculated the potential depth $V_{\Sigma N(I=1/2)}^C(^3S)$ for the 3S state through $\mathbf{p} = 0$ Wigner transform of the non-local exchange kernel. We find $V_{\Sigma N(I=1/2)}^C(^3S) = -38$ MeV, -24 MeV, and -18 MeV for RGM-F, FSS, and RGM-H, respectively. This corresponds to the contributions from the $\Sigma N(I = 1/2)$ $^3S_1 + ^3D_1$ channel in Table 2 very well; namely, -24.5 MeV, -20.7 MeV, and -17.9 MeV for RGM-F, FSS, and RGM-H, respectively. For the $\Sigma N(I = 1/2)$ $^1P_1 + ^3P_1$ contribution, our quark model yields fairly large attraction of $-7 \sim -11$ MeV, in comparison with the meson-exchange potentials. This is again by the strong effect of the $LS^{(-)}$ force in our quark model. Tables 1 and 2 show that the total strength of the Σ s.p. potential in our quark model has rather strong model dependence from -2 MeV to 20 MeV, as a cancellation of the repulsive $I = 3/2$ contribution and the attractive $I = 1/2$ contribution. It seems to be very important to determine the isospin dependence of the Σ s.p. potential, as is suggested in [39].

The analysis [40] of the energy shifts and the widths of Σ^- atomic levels in 1970's concluded that the Σ s.p. potential is attractive $-\text{Re } V_{opt}^\Sigma(0) \sim 25 - 30$ MeV. The DWIA analysis [41] of the pion inclusive spectra, which is related to the Σ -formation in (K^-, π^+) reaction, suggests that the Σ potential is much weaker. The G -matrix calculation with the NSC89 potential, using a continuous choice of s.p. potentials, predicts the depth of about 15 MeV [20]. The calculations in [18] and [19] indicate⁵ that the Nijmegen model D gives a similar attractive potential. On the other hand, the Nijmegen model F seems to predict a repulsive s.p. potential. The origin of 5.8 MeV repulsion, reported in [19] for the model F is again the $\Sigma N(I = 3/2)$ $^3S_1 + ^3D_1$ channel, which gives a strongly repulsive contribution of 47.1 MeV, comparable to our value 48.3 MeV in Table 1. An attempt [21] to extend a relativistic mean-field theory to Σ -hypernuclei predicted almost the same s.p. energy for the Λ and Σ , indicating that the Σ potential is as attractive as the Λ one. In the relativistic mean field description, calculated results depend on the ratio of the coupling constants $\alpha_i \equiv (g_{i\Sigma^0}/g_{iN})$ ($i = \sigma, \omega, \rho$). The quark-meson coupling model [42] also gave similar results.

In the mean time, the Σ^- atomic data were reanalyzed [17], allowing more general density-dependence. This study indicates that the Σ potential is re-

⁵ A QTQ choice with introducing the constant shift in the energy denominator was used in these calculations [18] and [19].

pulsive inside the nucleus. Guided by this observation, it was shown [23] that the tuning of the ratio of the coupling constants α_i can produce the repulsive Σ potential. Dabrowski [39] showed that the recent (K^-, π^\pm) experiments at BNL [43] favor the repulsive Σ potential, the strength of which is about 20 MeV. It is interesting to see that our FSS quark-model result is in line with these recent observations. However, it should be noted that as in the case of the Λ particle the potential at $k_F = 1.35 \text{ fm}^{-1}$ may not be directly related to the empirical s.p. potential. The density and starting-energy dependences must be taken into account.

In early pioneering stage of the sigma-hypernuclear formation experiments [44], the observed spectra hinted narrow peak structure for the Σ -formation even if they are in unbound energy region. Thus the calculation of the Σ width in nuclear medium was paid much attention. In recent experiments [43], however, no narrow peaks were reported. In our calculation, the Σ s.p. potential is repulsive and the Σ bound state is unlikely except for the specific light nuclei, where the spin-isospin dependence can produce Σ bound states like the $^4_\Sigma \text{He}$ [45]. If the Σ s.p. potential is repulsive, the strength of the imaginary part of the s.p. potential is not related to the spreading width of the Σ formation peaks. The k -dependence of the imaginary Σ s.p. potential is shown in Fig. 4. The value of about 20 MeV near $k = 0$ at $k_F = 1.35 \text{ fm}^{-1}$ is in accord with the calculation by Schulze *et al.* [20].

5 Summary

We have presented the first attempt to apply the recent realistic quark-model baryon-baryon interaction to nuclear matter calculations. The reaction matrices for the NN , ΛN and ΣN channels have been calculated in ordinary nuclear matter by solving the Bethe-Goldstone equations for the exchange kernel of the quark-model interaction. We used mainly the interaction called FSS, which was developed by Kyoto-Niigata group [5–9]. Since the quark model provides a unified framework to describe the NN and YN interactions, it is very interesting to study the predictions for hyperon properties in nuclear medium in this model.

The quark-model interaction is defined in formulating the RGM equation for the relative wave function of the (3q)-(3q) clusters. Thus we have to first define partial wave amplitudes in momentum space by numerical angular integration of the quark exchange kernel. Then self-consistent determination of the NN , ΛN and ΣN G -matrices in nuclear matter is straightforward.

In the nucleon sector the FSS gives similar saturation properties for the nuclear matter as other realistic NN potentials. This result is probably non-

trivial but interesting, in view of the fact that the origin and the description of the short-range part of the interaction is quite different. The Λ single-particle (s.p.) potential has the depth of about 46 MeV in the case of the continuous prescription for intermediate energy spectra. This value is slightly more attractive than the value expected from the experimental data of Λ -hypernuclei [16]. The Σ s.p. potential has turned out to be repulsive with the strength of about 20 MeV, the origin of which is traced back to the strong Pauli repulsion in the $\Sigma N(I = 3/2) \ ^3S_1$ state. This result seems to be consistent with the indication from the analysis by Dabrowski [39] of recent (K^-, π^\pm) experiments [43] at BNL. Future experiments will be expected to settle the problem of the Σ s.p. potential.

Our calculation also indicates that the FSS is not appropriate for predicting the asymptotic behavior of s.p. potentials in high-momentum region [28]. The present NN two-body potential is not designed for the application to such a high-energy region. It would be interesting to examine how the prediction of the model FSS is changed by introducing momentum-dependent higher-order terms involved in the S-meson exchange central force. The improvement in this direction is now under way.

The $LS^{(-)}$ force is absent in the NN interaction, but it plays a characteristic role in the YN interaction. In fact, the quark-model interaction suggests an important antisymmetric spin-orbit component. Thus the examination of the combined effects of the LS and $LS^{(-)}$ interactions to the hyperon s.p. spin-orbit potential is very interesting. In the present paper, however, we did not discuss this problem. This subject is studied in a separate paper [26].

Finally we note that it will be an important future subject to consider hyperonic nuclear matter in the scope of the quark-model baryon-baryon interaction, since the study of $\Lambda\Lambda$ and ΞN interactions is also in progress [46]. Since the Σ s.p. potential is repulsive in the quark-model description, the admixture of the Σ particle is suppressed and this, in turn, will affect the behavior of the Λ particles in dense hyperonic nuclear matter.

References

- [1] M. Oka and K. Yazaki, in *Quarks and Nuclei*, ed. W. Weise (World Scientific, Singapore, 1984), p.489; K. Shimizu, Rep. Prog. Phys. **52** (1989) 1; C. W. Wong, Phys. Rep. **136** (1986) 1.
- [2] Y. Fujiwara, Prog. Theor. Phys. Suppl. No. 91 (1987), 160.
- [3] C. Nakamoto, Y. Suzuki and Y. Fujiwara, Prog. Theor. Phys. **94** (1995) 65.

- [4] Y. Fujiwara, C. Nakamoto and Y. Suzuki, *Prog. Theor. Phys.* **94** (1995) 215 and 353.
- [5] Y. Fujiwara, C. Nakamoto and Y. Suzuki, *Phys. Rev. Lett.* **76** (1996) 2242.
- [6] Y. Fujiwara, C. Nakamoto and Y. Suzuki, *Phys. Rev.* **C54** (1996) 2180.
- [7] T. Fujita, Y. Fujiwara, C. Nakamoto, Y. Suzuki, T. Yamamoto and R. Tamagaki, *Prog. Theor. Phys.* **96** (1996) 463.
- [8] T. Fujita, Y. Fujiwara, C. Nakamoto and Y. Suzuki, *Prog. Theor. Phys.* **96** (1996) 653.
- [9] T. Fujita, Y. Fujiwara, C. Nakamoto and Y. Suzuki, *Prog. Theor. Phys.* **100** (1998) 931.
- [10] M. M. Nagels, Th. A. Rijken and J. J. de Swart, *Phys. Rev.* **D15** (1977) 2547.
- [11] M. M. Nagels, Th. A. Rijken and J. J. de Swart, *Phys. Rev.* **D20** (1979) 1633.
- [12] P. Maessen, Th. A. Rijken and J. de Swart, *Phys. Rev.* **C40** (1989) 2226.
- [13] Th. A. Rijken, V. G. J. Stoks and Y. Yamamoto, *Phys. Rev.* **C59** (1999) 21.
- [14] B. Holzenkamp, K. Holinde and J. Speth, *Nucl. Phys.* **A500** (1989) 485.
- [15] A. Reuber, K. Holinde and J. Speth, *Nucl. Phys.* **A570** (1994) 543.
- [16] H. Bando, T. Motoba and J. Žofka, *Int. J. of Mod. Phys.* **A21** (1990) 4021.
- [17] C. J. Batty, E. Friedman and A. Gal, *Phys. Lett.* **B335** (1994) 273; *Phys. Rep.* **287** (1997) 385.
- [18] Y. Yamamoto and H. Bando, *Prog. Theor. Phys.* **73** (1985) 905.
- [19] Y. Yamamoto and H. Bando, *Prog. Theor. Phys.* **83** (1990) 254.
- [20] H.-J. Schulze, M. Baldo, U. Lombardo, J. Cugnon and A. Lejeune, *Phys. Rev.* **C57** (1998) 704.
- [21] M. Rufa, J. Schaffner, J. Maruhn, H. Stöcker, W. Greiner and P.-G. Reinhard, *Phys. Rev.* **C42** (1990) 2469.
- [22] N. K. Glendenning, D. Von-Eiff, M. Haft, H. Lenske and M. K. Weigel, *Phys. Rev.* **C48** (1993) 889.
- [23] J. Mareš, E. Friedman, A. Gal and B. K. Jennings, *Nucl. Phys.* **A594** (1995) 311.
- [24] K. A. Brueckner, C. A. Levinson and H. M. Mahmoud, *Phys. Rev.* **95** (1954) 217; K. A. Brueckner and C. A. Levinson, *Phys. Rev.* **97** (1955) 1344.
- [25] B. D. Day, *Rev. Mod. Phys.* **39** (1967) 719.
- [26] Y. Fujiwara, M. Kohno, T. Fujita, C. Nakamoto and Y. Suzuki, submitted to *Nucl. Phys.* **A** (1999).

- [27] Y. Fujiwara, C. Nakamoto and Y. Suzuki and Zhang Zong-ye, *Prog. Theor. Phys.* **97** (1997) 587.
- [28] Y. Fujiwara, M. Kohno, T. Fujita, C. Nakamoto and Y. Suzuki, submitted to *Prog. Theor. Phys.* (1999).
- [29] M. I. Haftel and F. Tabakin, *Nucl. Phys.* **A158** (1970) 1.
- [30] M. Lacombe, B. Loiseau, J. Richard, R. Vinh Mau, J. Côté, P. Pirès and R. de Tourreil, *Phys. Rev.* **C21** (1980) 861.
- [31] R. Machleidt, *Adv. Nucl. Phys.* **19** (1989) 189.
- [32] R. Brockmann and R. Machleidt, *Phys. Rev.* **C42** (1990) 1965.
- [33] Y. Fujiwara, T. Fujita, C. Nakamoto, Y. Suzuki and M. Kohno, *Nucl. Phys.* **A639** (1998) 41c.
- [34] S. Shinmura, Y. Akaishi and H. Tanaka, *Prog. Theor. Phys.* **71** (1983) 546.
- [35] Y. Yamamoto, T. Motoba, H. Himeno, K. Ikeda and S. Nagata, *Prog. Theor. Phys. Suppl.* No. 117 (1994) 361.
- [36] E. Hiyama *et al.*, private communication.
- [37] T. Hasegawa *et al.*, *Phys. Rev.* **C53** (1996) 1210.
- [38] Y. Fujiwara, C. Nakamoto, T. Fujita, Y. Suzuki and M. Kohno, in *Proceedings of the XVII RCNP International Symposium on Innovative Computational Methods in Nuclear Many-Body Problems (INNOCOM97)*, ed. H. Horiuchi, M. Kamimura, H. Toki, Y. Fujiwara, M. Matsuo and Y. Sakuragi, (World Scientific, Singapore, 1998), p. 295.
- [39] J. Dabrowski, *Phys. Rev.* **C60** (1999) 025205.
- [40] C.J. Batty, *Phys. Lett.* **B87** (1979) 324; *Nucl. Phys.* **A372** (1981) 433.
- [41] M. Kohno, R. Hausmann, P. Siegel and W. Weise, *Nucl. Phys.* **A470** (1987) 609.
- [42] K. Tsushima, K. Saito, J. Haidenbauer and A.W. Thomas, *Nucl. Phys.* **A630** (1998) 691.
- [43] R. Sawafta, *Nucl. Phys.* **A585** (1995) 103c; **A639** (1998) 103c.
- [44] R. Bertini *et al.*, *Phys. Lett.* **B90** (1980) 375; **B136** (1984) 29; **B158** (1985) 19.
- [45] T. Harada and Y. Akaishi, *Phys. Lett.* **B262** (1991) 205.
- [46] C. Nakamoto, Y. Suzuki and Y. Fujiwara, *Prog. Theor. Phys.* **97** (1997) 761.